Cooperative Underwater Manipulation Systems: Control Developments within the MARIS project

Giuseppe Casalino, Enrico Simetti, Ninad Manerikar, Alessandro Sperinde, Sandro Torelli and Francesco Wanderlingh

University of Genova, Via Opera Pia 13, Italy(e-mail: pino@dist.unige.it)

Abstract: A novel co-operative control algorithm has been presented in this paper for the transportation of large objects in underwater scenarios using two free floating vehicles, each one endowed with a 7 d.o.f redundant manipulator. The paper also gives detailed information about the theoretical foundations related to the kinematic and dynamic modelling, and then to the cooperative control, of the overall system. Due to the low bandwidth in underwater scenarios, the algorithm presented in the paper just exchanges six numbers (tool frame velocities) and still gives extremely good results even with such high limitations on the information exchange.

1. INTRODUCTION

Research in the field of Autonomous Underwater Robotics and Manipulation has come a long way from a technological as well as from an algorithmic point of view in the past two decades. European projects including AMADEUS [5], ALIVE [1], SAUVIM [2] have successfully demonstrated autonomous manipulation capabilties. Then, within the recently concluded EU-funded project TRIDENT [4], more enhanced control capabilities for autonomous floating vehicle-arm systems, also including operational effectiveness aspects to be exhibited in terms of agility of the overall system, were finally achieved for vehicles and arms of comparable masses and inertias; and within a unifying, functional and algorithmic, control and coordination framework [4]. Keeping these advancements in mind , the idea of further investigating the possibility of having a team of underwater robots performing cooperative manipulation and transportation certainly springs up to the surface. To this regard, the national Italian project MARIS [3] has been launched recently whose main aim is to develop state of the art co-operative control algorithms and technology as well as experimental proof of concept trial, clearly demonstrating the fact that cooperative intervention tasks can be successfully carried out in harsh underwater scenarios. Within this context, the contribution of this paper is the development, within a unified framework, of a cooperative control policy relevant to both the involved mission phases i.e transportation, then followed by the final positioning of the shared object grasped by two agents, as shown in Fig. 1. To these aims, the paper is structured as follows. Section 2 briefly recalls the already unifying framework for single agents [4], capable of handling equality and inequality objectives; while Section 3 will extend the approach to the mentioned decentralized multi objective constrained co-operative control problem. Section 4 will deal the dynamic modelling and control of the overall system while the simulation results supporting the proposed approach will be then presented in section 5. Finally, some conclusions and foreseen future works will be discussed in section 6.

* This work has been supported by MIUR(Ministry of Education, University and Research) within the PRIN project MARIS, prot. 2010FBLHRJ project.

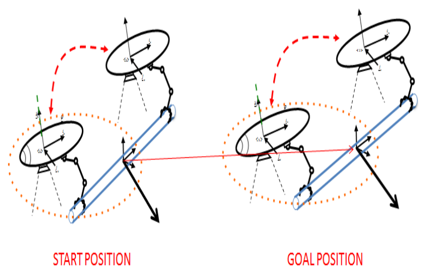

Fig. 1. Transportation and Positioning Phase

2. TASK-PRIORITY BASED COORDINATED CONTROL FOR INDIVIDIAL FLOATING MANIPULATION

For individual floating manipulation systems [4], a task-priority based framework [6] has been adopted where each task can be assigned a priority according to its importance; and where the various tasks (maintaining the joint limits, keeping manipulanility above a certain threshold etc.) are therefore solved according to their priority in a descending order, meaning that the highest priority task is solved first and then the solutions of the other tasks are solved inside the kernel subspace of the higher priority ones. The task priority paradigm has been implemented in various fields of robotics:mobile manipulators such as [9], [10]; multiple coordinated mobile manipulators [11] as well as in humanoid robots [12],[13]. An extension of the task-priority framework has been developed in [4], where suitable activation functions are used for the activation and deactivation of the equality as well as inequality tasks. One of the major advantages of this method is that when a task disappears from the priority list it results in an enlargement of the mobility space which in turn is favorable to the lower priority tasks.

2.1 Individual Control Objectives

This susbsection gives details about the control objectives (equality as well as inequality) listed in the order of their priority (first task with highest priority and so on) that generally need to be considered for an individually operating system.

(1) Joint Limits: This is an inequality type task used to maintain the joints within well defined bounds in order to maintain safety and good operability of the arm.
(2) Manipulability: This inequality type objective is used in order to guarantee the arm operating with a good dexterity, the arm itself must also keep its manipulability measure [7] above a minimum value.
(3) Horizontal Attitude: The vehicle should stay at an almost horizontal attitude established by bounds on its pitch angle.
(4) Camera centering for object transportation: This objective is activated during the transportation phase, and requires the goal frame grossly maintained within the visual cone of the endowed forward-looking camera.
(5) Camera centering for object positioning: This task is activated during the final positioning phase and requires the grasped object frame and the goal one both maintained in the field of view of the endowing positioning camera.
(6) Positioning camera distance and height: This objective is activated during the positioning phase and requires the positioning camera to be above a certain height and below a certain horizontal distance from the goal frame; in order to enable the best operability conditions for the positioning camera.
(7) Grasped object positioning: This objective is active during both the transportation and final positioning phase. It requires the grasped object frame approaching the goal one, still to be exactly positioned on it.
(8) Vehicle motion minimality: Since the vehicle generally exhibits a larger mass and inertia than the arm, during the final positioning phase it is advisable to have it move, only the strict necessary amount needed for accomplishing the related tasks. Thus always favoring the use of the arm whenever possible,in any situation, depending on the task status (active or not active).

2.2 Algorithmic structure of the prioritized control law

Consider the absolute velocity exhibited by the tool-frame $< t >$ (i.e.the grasped object frame), represented by the stacked vector of its linear and angular absolute velocities, each one assumed with components on $< t >$ itself, which can be expressed as:

$$\dot{x} = J\dot{q} + Sv \doteq H\dot{y} \tag{1}$$

where $\dot{q}$ represents the arm joint velocity, v represent the vehicle velocity, each one with components on frame $< t >$; while matrices J and S respectively represent the arm and vehicle Jacobian matrices projected on frame $< t >$; with the second one (i.e matrix S) simply corresponding to the existing non-singular rigid body velocity transformation from frame $< v >$ to frame $< t >$, at the current arm posture. Moreover the stacking of vectors $\dot{q}$ and v into vector $\dot{y}$ represents the system-velocity vector, directly related with $\dot{x}$ via the resulting overall tool-frame Jacobian matrix $H \doteq [J, S]$. By now assuming a fully actuated vehicle (i.e. exhibiting $v \in R^6$) we can then see how, under this sole assumption, H turns out to be full-row rank; meaning that $\text{Span}(H) = R^6$ and consequently $\dot{x}$ can span the entire 6-dimensional space. Then, $\dot{y}$ is represented in the following (redundant) classical parameterized form

$$\dot{y} = H^{\#}\dot{x} + (I - H^{\#}H)\dot{z} \doteq M\dot{x} + Q\dot{z} \tag{2}$$

Taking in to account the above assumptions, it can be noted that, within equation (2), more precisely we have $Span(M) = R^6$; $Span(Q) = R^{n-6}$; $Span(M) \perp Span(Q)$; $HM = I$ and $HQ = 0$. The first, second and the fourth conditions result as direct consequence of the vehicle full actutation assumption, whereas the others are standard for any represention of the form shown in equation (2). The above representation will turn out to be very useful for analyzing the kinematic effects introduced by the external equality constraints which will arise, when two systems of the above type are firmly holding a shared object, to be cooperatively manipulated or transported. With reference to the above introduced relationship, the prioritized control law develops, at each time instant, via the execution of the following two sequential algorithmic runs:

a) First run (Tool-frame velocity conditioning): With the tool-frame velocity vector ($\dot{x}$) assigned as a dummy vector parameter, the sequence of prioritized tasks is optimized with respect to the null-space system velocities by using the same algorithmic structure of [4]; thus formerly leading to the following conditionally optimal null-space system velocity linear control law:

$$\dot{z} = \dot{\rho} + P\dot{x} \tag{3}$$

Where $\dot{\rho}$ is the conditionally optimal null-space system velocity reference for a null tool-frame velocity conditioning; while the additional term $P\dot{x}$ leads to conditional optimality for any non-zero tool-frame velocity parametrization.

b) Second run (Tool-frame velocity optimization): With the vector $\dot{z}$ constrained to obey to the above control law, the sequence of prioritized tasks is then optimized with respect to the tool-frame velocity vector parameter $\dot{x}$ by still using the same algorithmic structure of [4]; thus finally leading to the following globally optimal null-space velocity:

$$\dot{\bar{z}} = \dot{\rho} + P\dot{\bar{x}} \tag{4}$$

where $\dot{\bar{x}}$ is the optimal value for the tool-frame velocity vector parameter. Then, by substituting equation (4) in equation (2), the optimal system velocity vector $\dot{\bar{y}}$ is consequently obtained as:

$$\dot{\bar{y}} = M\dot{\bar{x}} + Q\dot{\bar{z}} \tag{5}$$

3. EXTENSION TO COOPERATIVELY OPERATING UNDERWATER FLOATING MANIPULATORS

Once the two floating manipulators have firmly grasped a shared object, as indicated in Fig.1, the problem of transporting the object, and finally positioning its attached frame $< t >$ on the goal frame $< g >$, has to be now solved within the set of system velocities $\dot{y}_a$, $\dot{y}_b$ characterized by the following parametrization:

$$\dot{y}_a = M_a\dot{x} + Q\dot{z}_a \quad (6)$$

$$\dot{y}_b = M_b\dot{x} + Q\dot{z}_b \quad (7)$$

with a common arbitrary tool-frame velocity $\dot{x}$ and separately arbitrary null space system-velocities $\dot{z}_a$ and $\dot{z}_b$.

In the cooperative scenario, an additional task of maintaining a given distance between the two vehicles will be introduced in order to avoid collisions. The cooperative control problem might actually be optimally solved by simply extending the application of previously outlined task priority based individual control law in the following way:

a) Independent first runs (Separate tool-frame velocity conditioning): At each time instant each system independently determines its own conditionally optimal null space system velocity control law, by optimizing its own list of prioritized tasks as if it were the sole agent acting on the object; thus separately obtaining (i.e. in a fully decentralized way) the following couple of separate conditionally optimal null space system velocity control laws:

$$\dot{z}_a = \dot{\rho}_a + P_a\dot{x}_a \quad (8)$$

$$\dot{z}_b = \dot{\rho}_b + P_b\dot{x}_b \quad (9)$$

With $\dot{x}_a$, $\dot{x}_b$ representing the corresponding tool-frame velocity dummy parametrization for each system.

b) Global second run (Tool-frame velocity optimization): By setting the common parametrization $\dot{x}_a \doteq \dot{x}_b \doteq \dot{x}$, the second optimization run for a common $\dot{x}$ should be now performed on a global basis by merging the separate lists of tasks into a whole superset of tasks (allowing a complete exchange of information which must include the task lists, the above devised conditioned control laws, as well as the configuration state of each system and all relevant Jacobian matrices). This would consequently lead to the optimal common tool frame velocity $\dot{x}^\circ$, that consequently will impose the following globally optimal null-space system-velocities:

$$\dot{z}_a^\circ = \dot{\rho}_a + P_a\dot{x}^\circ \quad (10)$$

$$\dot{z}_b^\circ = \dot{\rho}_b + P_b\dot{x}^\circ \quad (11)$$

And consequently the overall optimal system-velocities $\dot{y}_a^\circ$, $\dot{y}_b^\circ$ by substituting equations (10), (11) into equations (6), (7) become of the form :

$$\dot{y}_a^\circ = M_a\dot{x}^\circ + Q_a\dot{z}_a^\circ \quad (12)$$

$$\dot{y}_b^\circ = M_b\dot{x}^\circ + Q_b\dot{z}_b^\circ \quad (13)$$

Since the above outlined global second run would actually require an excessive amount of data exchange between the agents, it generally turns out to be practically unfeasible, especially within the case considered here of underwater interventions, where low-bandwidth acoustic communication channels typically are the sole available means for data exchanges. As a consequence of the above consideration, clearly forcing us to renounce the global optimality, the following suboptimal procedure, however based on a reduced amount of information to be exchanged, can be therefore proposed:

a) Independent first & second runs (Separate optimizations): At each time instant each system independently performs its own global optimization, as if it were the sole agent acting on the grasped object; thus formerly obtaining the following couple of individually unconditioned optimal null-space system velocities:

$$\dot{\bar{z}}_a = \dot{\rho}_a + P_a\dot{\bar{x}}_a \quad (14)$$

$$\dot{\bar{z}}_b = \dot{\rho}_b + P_b\dot{\bar{x}}_b \quad (15)$$

b) Tool frame velocities exchange & fusion policy: At each time instant the separately evaluated individually optimal tool-frame velocities $\dot{\bar{x}}_a$, $\dot{\bar{x}}_b$ are exchanged (this requires the transmission of solely six numbers in both directions) and a common value $\dot{\hat{x}}$ is determined as the result of an apriori agreed fusion policy. Quite simply such fusion policy may trivially be the mean value between $\dot{\bar{x}}_a$, $\dot{\bar{x}}_b$ or more generally a suitable convex combination of them; or even more sophisticated fusion policies whose devising is however still the subject of further investigations. In a broader sense, it should be noted that such convex combinations could be used where one system can be the leader and the other system can be the follower and they can even smoothly change the role depending on the scenario.

c) Null-Space velocity retuning: At each time instant each system simply retunes, via trivial substitution into equations (8) & (9), its null-space system velocity references to the so established conditioning common tool-frame velocity value, thus obtaining the following couple of separate conditionally optimal null space system velocity references:

$$\dot{\hat{z}}_a = \dot{\rho}_a + P_a\dot{\hat{x}} \quad (16)$$

$$\dot{\hat{z}}_b = \dot{\rho}_b + P_b\dot{\hat{x}} \quad (17)$$

Each one characterized by the common tool-frame velocity vector $\dot{\hat{x}}$. Then the conditionally optimal system velocities $\dot{\hat{y}}_a, \dot{\hat{y}}_b$ are recomputed via equations (6) & (7), now leading to:

$$\dot{\hat{y}}_a = M_a\dot{\hat{x}} + Q_a\dot{\hat{z}}_a \quad (18)$$

$$\dot{\hat{y}}_b = M_b\dot{\hat{x}} + Q_b\dot{\hat{z}}_b \quad (19)$$

The main idea behind proposing the above solution, is not only to estabilish a common tool-frame velocity (as required by the firm grasping constraints) but also to resort to the common tool-frame velocity which may be considered as reasonable compromise between two individual optimal values; in any case without requiring any unfeasible amount of information exchange between the agents.

As a matter of fact, further investigations are actually needed for measuring the degree of sub-optimality introduced by the employment of $\dot{\hat{x}}$ in lieu of the globally optimal one $\dot{x}^\circ$, which however remains (though almost impossible to be real-time evaluated within underwater environment) a reference stone with respect to which any suboptimal control law has to be compared.

Moreover the possible existence of secondary effects, if any, that might appear as a consequence of the introduced sub-optimality, are still to be investigated. However, the

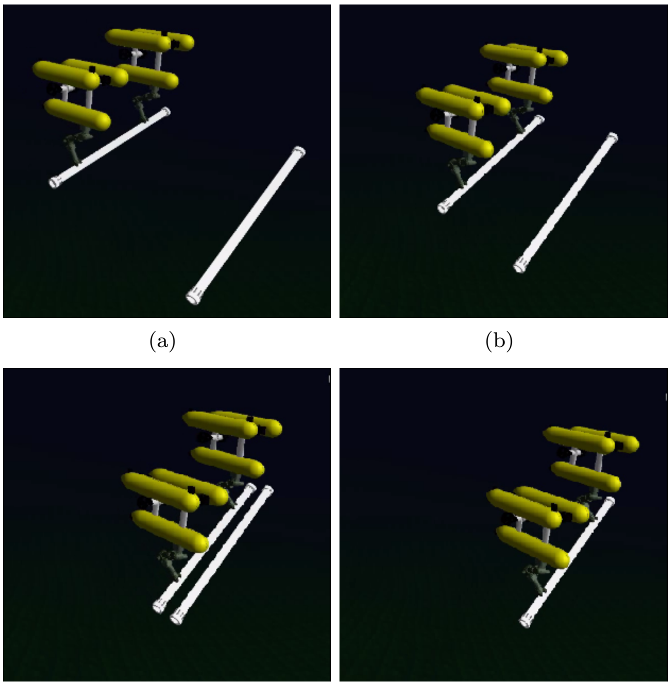

(a) (b) (c) (d)

Fig. 2. Different stages in the transportation and positioning phase

extensive simulations performed in the section 5 show encouraging results even by just using the arithmetic mean between $\dot{\bar{x}}_a$, $\dot{\bar{x}}_b$.

4. DYNAMIC MODELING AND CONTROL

In this section the dynamic model of the overall system has been obtained, which will be used for further developing the fully decentralized Dynamic Control layer.

4.1 Overall System Dynamic

The overall system dynamics [14] can be obtained by jointly considering the dynamic equations of the two vehicle-arm subsytems, the grasped object and by also considering the kinematic constraints. Thus they can be represented by the following set of DAE's (Differential Algebraic Equations) and are given below as follows:

$$A_a\ddot{y}_a + B_a\dot{y}_a + C_a = \mu_a - H_a^T f_a \quad (20)$$
$$A_b\ddot{y}_b + B_b\dot{y}_b + C_b = \mu_b - H_b^T f_b \quad (21)$$
$$A_c\ddot{x} + B_c\dot{x} + C_c = f_a + f_b \quad (22)$$
$$H_a\dot{y}_a = H_b\dot{y}_b = \dot{x} \quad (23)$$

where the equation (22) represents the object dynamic expressed with respect to its fixed frame $< t >$ which is subjected to the sum of force/torque actions f_a and f_b, both with components on the frame $< t >$. Obviously these forces/torques are exerted at the frame $< t >$ by the two vehicle subsystems under the assumption of firm grasping conditions. The equations (20) and (21) instead represent the dynamics of the vehicle-arm subsystems, respectively driven by the following set of actuation vectors $\mu_a \doteq \begin{bmatrix} m_a \\ \tau_a \end{bmatrix}$ & $\mu_b \doteq \begin{bmatrix} m_b \\ \tau_b \end{bmatrix}$, where m_a,m_b represent the corresponding arm joint torque vector; whereas τ_a, τ_b represent the force/torque vectors resulting from the correponding set of vehicle thrusters and acting at the corresponding vehicle frames ¡v_a¿ and ¡v_b¿, where they are respectively projected. Now the stacked vector i.e col(f_a, f_b) of the force/torques acting at frame $< t >$ is further decomposed into two orthogonal components. These components represent the so-called motion and internal force/torques which are simply the minimal norm set of those force/torques producing the resultant, plus the orthogonal set of those force/torques without any resultant. This decompostion results in:

$$f_a = r + \zeta \quad (24)$$
$$f_b = r - \zeta \quad (25)$$

where: $r = \frac{1}{2}(f_a + f_b)$ and $\zeta = \frac{1}{2}(f_a - f_b)$
Thus 2r is the induced resultant at frame $< t >$ and $\pm\zeta$ is the associated internal force/torque system oppositely acting on the object at the same frame. Thus, by substituting equations (24), (25) into equations (20), (21), (22), (23) the following equivalent dynamic model is obtained as shown below:

$$A_a\ddot{y}_a + B_a\dot{y}_a + C_a = \mu_a - H_a^T r - H_a^T\zeta \quad (26)$$
$$A_b\ddot{y}_b + B_b\dot{y}_b + C_b = \mu_b - H_b^T r + H_b^T\zeta \quad (27)$$
$$A_c\ddot{x} + B_c\dot{x} + C_c = 2r \quad (28)$$
$$H_a\dot{y}_a = H_b\dot{y}_b = \dot{x} \quad (29)$$

The above equations clearly highlight the fact that the object motion effort which is represented by the resultant 2r can be interpreted as equally shared by the two vehicle-arm subsytems. Thus, the tool frame of each system is subjected to half of the total resultant 2r; which is actually one of the noteworthy reasons for a transportation to be carried out in a cooperative sense. Meanwhile the same equations show how the internal force/torque system $\pm\zeta$, however oppositely reflect on the tool frames of the two subsytems. Then, by substituting the equation (28) into the equations (26) and (27), the following dynamic model is obtained

$$A_a\ddot{y}_a + B_a\dot{y}_a + C_a + \frac{1}{2}H_a^T(A_c\ddot{x} + B_c\dot{x} + C_c) = \mu_a - H_a^T\zeta \quad (30)$$

$$A_b\ddot{y}_b + B_b\dot{y}_b + C_b + \frac{1}{2}H_b^T(A_c\ddot{x} + B_c\dot{x} + C_c) = \mu_b + H_b^T\zeta \quad (31)$$

$$H_a\dot{y}_a = H_b\dot{y}_b = \dot{x} \quad (32)$$

The above equations can also be equivalently interpreted as if the two systems were loaded separately, at their corresponding end-effector, by just half of the grapsed object (i.e as if the end-effector link of each system actually have mass and inertia that is augmented by half of that of the object); and then constrained to exhibit the same velocity $\dot{x}$ at such dynamically augmented end-effectors. In fact, by representing $\ddot{x}$, $\dot{x}$ as imposed by the kinematic constraints in the respective equations, we eventually get the following final model as shown below:

$$(A_a + \frac{1}{2}H_a^T A_c H_a)\ddot{y}_a + (B_a + \frac{1}{2}H_a^T B_c H_a + A_c\dot{H}_a)\dot{y}_a + (C_a + \frac{1}{2}H_a^T C_c) = \mu_a - H_a^T\zeta \quad (33)$$

$$(A_b + \frac{1}{2}H_b^T A_c H_b)\ddot{y}_b + (B_b + \frac{1}{2}H_b^T B_c H_b + A_c \dot{H}_b)\dot{y}_b + (C_b + \frac{1}{2}H_b^T C_c) = \mu_b + H_b^T \zeta \quad (34)$$

$$H_a \dot{y}_a = H_b \dot{y}_b \quad (35)$$

where the effects induced by the half-body, loading the end-effector of each system, now appear embedded within the resulting generalized coordinate representation of each one of them. The model described above can be further represented in a more compact form as shown below:

$$\bar{A}_a \ddot{y}_a + \bar{B}_a \dot{y}_a + \bar{C}_a = \mu_a - H_a^T \zeta \quad (36)$$

$$\bar{A}_b \ddot{y}_b + \bar{B}_b \dot{y}_b + \bar{C}_b = \mu_b + H_b^T \zeta \quad (37)$$

$$H_a \dot{y}_a = H_b \dot{y}_b \quad (38)$$

or in the even more compact form as given below:

$$\bar{A}\ddot{y} + \bar{B}\dot{y} + \bar{C} = \mu - G^T \zeta \quad (39)$$

$$G\dot{y} = 0 \quad (40)$$

where: Matrix $\bar{A}$ = diag($\bar{A}_a$, $\bar{A}_b$), Matrix $\bar{B}$ = diag($\bar{B}_a$, $\bar{B}_b$), $\bar{C}$ = col($\bar{C}_a$, $\bar{C}_b$) & G = row(H_a,-H_b). The above overall system dynamic equivalent model representations will be the ones used for devising the fully decentralized Dynamic Control Layer (DCL) within the next subsection.

4.2 Decentralized Dynamic Control

Consider the global system reference velocity vectors $\dot{\bar{y}}$, whose components $\dot{\bar{y}}_a$, $\dot{\bar{y}}_b$ are separately made available to the dynamic controllers of the corresponding system, each one consistent with the kinematic contraints, as established by the adoption of a common tool-frame reference velocity as described in the previous section. Then, in order to track the system velocity reference signal $\dot{\bar{y}}$ let us now introduce the following constrained positive definite quadratic form as a candidate lyapunov function

$$V \doteq \frac{1}{2}\delta\dot{\bar{y}}^T \bar{A} \delta\dot{\bar{y}} \quad (41)$$

$$G\dot{y} = 0 \quad (42)$$

where: $\delta\dot{\bar{y}} \doteq \dot{y} - \dot{\bar{y}}$

The constraint equation (42) derives from the fact that $\dot{y}$ is congruent with the constraints, as imposed by the system physics and $\dot{\bar{y}}$ is the global reference system velocity vector which is constructed to be congruent (upon tool-frame reference velocities exchange and use of a fusion policy, as described in the previous section). Moreover, the positive definite property of this quadratic form arises from the positive defininition of matrix $\bar{A}$ and from the fact that constraining its arguments within a linear manifold (even if time varying) does not alter this positive definite property. The existing analytical advantages in choosing a candidate Lyapunov function of the above form rather than a simpler one, will appear in the following. In fact, by differentiating equation (41) with respect to time along equation (39), after some simple algebra we get

$$\begin{aligned} \dot{V} &= \delta\dot{\bar{y}}^T(\mu - \bar{A}\ddot{\bar{y}} - \bar{B}\dot{y} - \bar{C} - G^T\zeta) + \frac{1}{2}\delta\dot{\bar{y}}^T \dot{\bar{A}} \delta\dot{\bar{y}} \\ &= \delta\dot{\bar{y}}^T(\mu - \bar{A}\ddot{\bar{y}} - \bar{B}\dot{\bar{y}} - \bar{C} - G^T\zeta) + \delta\dot{\bar{y}}^T \bar{B} \delta\dot{\bar{y}} \\ &= \delta\dot{\bar{y}}^T(\mu - \bar{A}\ddot{\bar{y}} - \bar{B}\dot{\bar{y}} - \bar{C}) \\ G\dot{y} &= 0 \end{aligned} \quad (43)$$

The second line in the equation (43) has been obtained by exploiting the well known property $z^T \bar{B} z = \frac{1}{2} z^T \dot{\bar{A}} z; \forall \dot{z}$. Then the final one in the third line has been obtained by exploiting the fact that $\delta\dot{\bar{y}}^T G^T \zeta = 0$ because of the constraint expressed in (42).

In the above equation (43) we can initially use part of the control μ for compensating the referenced Coriolis forces, the gravitational forces and the referenced accelerations, by actually separately acting on each system, thanks to the structure of the involved matrices (as defined at the end of the previous subsection). Thus we obtain:

$$\dot{V} = \delta\dot{\bar{y}}^T u \quad (44)$$

$$G\dot{y} = 0 \quad (45)$$

Then, by letting the residual part of the control be, it is also of the decentralized form

$$u = -\gamma\delta\dot{\bar{y}}; (\gamma > 0) \quad (46)$$

and we can actually make

$$\dot{V} = -\gamma\delta\dot{\bar{y}}^T \delta\dot{\bar{y}} < 0 \quad (47)$$

$$G\delta\dot{\bar{y}} = 0 \quad (48)$$

which guarantees the asymptotic convergence of $\delta\dot{\bar{y}}$ towards zero, along the constraining subspace $G\delta\dot{\bar{y}} = 0$.

5. PRELIMINARY SIMULATION RESULTS

This section gives details about the preliminary simulation results obtained by using the algorithms described in the sections above. The goal of the simulation trials was to transport an object from an initial starting position to a final position assuming that the object is grasped, using two free-floating vehicles (6 d.o.f) endowed with two redundant manipulators(7 d.o.f). The tasks are in order of priority: keeping away from joint limits, keeping the manipulability measure above a certain threshold, maintaining the horizontal attitude of the vehicles, maintaining a fixed distance between the vehicles, reaching the desired goal position and minimizing the vehicle velocity. The tasks related to the camera have not been included in these preliminary simulations and will be added in the future. The two systems are commanded to transport the object 6 m along the x-axis, 2 m along the y-axis and 1 m along the z-axis. Therefore goal position of the object in xyz co-ordinates is (6,2,1) meters rotated by an angle of 30 degrees around the x-axis. UWSim [8], which is an underwater robotics simulator, has been used for performing visual rendering.

For these simulations we have used the activation functions as presented in [4], i.e. bell-shaped functions of the task variable with finite support. In particular, the activation function is equal to one whenever the corresponding inequality is not satisfied and it smoothly goes to zero whenever the variable is inside the region where the inequality is instead satisfied. The buffer zone where the activation function is greater than zero but the inequality is already satisfied serves the purpose of avoiding chattering phenomena.

Fig. 4 reports the time history of the activation functions for the joint limits, manipulability, horizontal attitude and distance between the vehicles tasks for the systems A & B. From figures 4(a), 4(b), 4(c), 4(d) it can be seen that different tasks are in transition during the trial

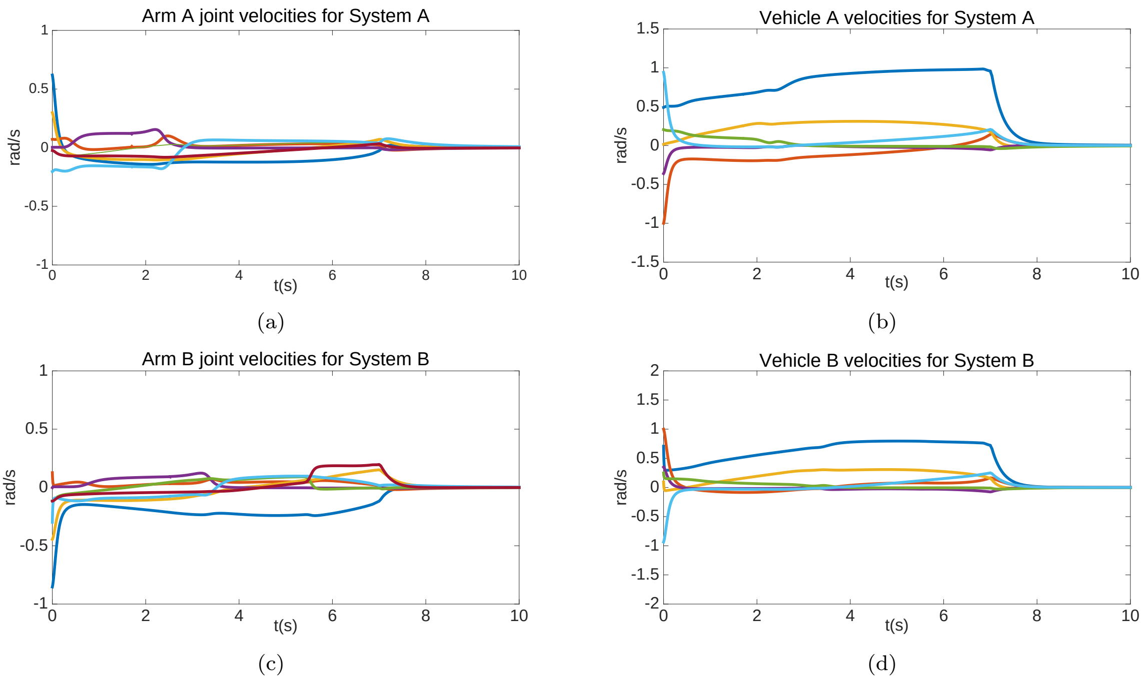

Fig. 3. Arm joint velocities and vehicle velocities of System A and B

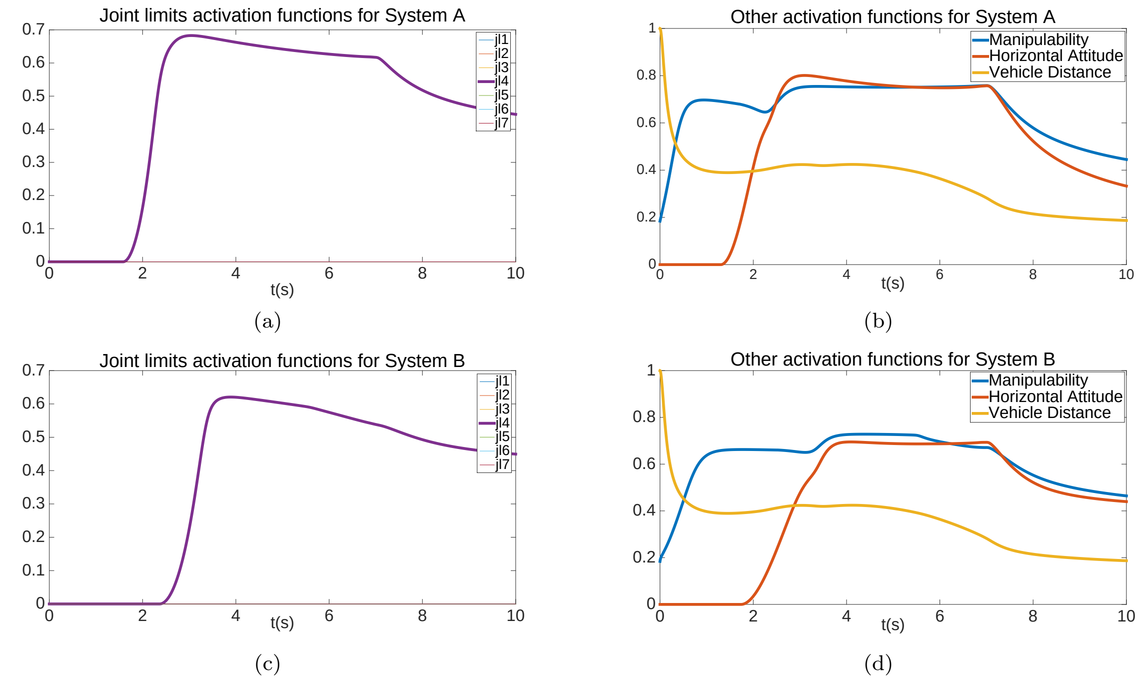

Fig. 4. Activation functions for System A and B

simulations. The proposed framework allows to maintain the corresponding variable of each task within its given boundaries using suitable smooth activation functions for activating and deactivating the tasks[4]. With this approach, the system manages to successfully accomplish the final objective of the mission, by transporting the object to the desired goal position as seen from the Fig. 2. The arm joint velocities and the vehicle velocities obtained during simulation for system A and system B in Fig. 3 shows the smoothness of the control that has been achieved.

6. CONCLUSION

In this paper we have presented a novel algorithm (which exchanges just 6 numbers at each time step) for the autonomous co-operative transportation of large objects by two free floating vehicles mounted with redundant manipulators. It also gives detailed information of the theoritical foundations, related to the kinematic and the dynamic modelling, and then to the cooperative control, of the overall system. One of the major challenges now would be to completely avoid the exchange of information between the agents. Since the arm and the vehicle operate at different control frequencies, the issue of multi-rate sampling still needs to be resolved and also the compensation of disturbances.

7. ACKNOWLEDGMENTS

This work has been supported by MIUR(Italian Ministry of Education, University and Reserach) through the ongoing MARIS project. The authors would like to thank the rest of the MARIS consortium which includes ISME (Integrated Systems for the Marine Environment);with the research units of the Universities of Genova, Pisa, Cassino and Southern Lazio, and of the University of Salento-Lecce;the research unit of the University of Parma; as well as the research unit of CNR-ISSIA in Genova, for their ongoing contributions on all other aspects and topics of the MARIS project.

REFERENCES

[1] Marty, P. ALIVE:An Autonomous Light Intervention Vehicle. Deep Offshore Technology Conference, France, (Nov 2003).

[2] J. Yuh, S. K. Choi, C. Ikehara, G. H. Kim, G. McMurty, M. Ghasemi-Nejhad, N. Sarkar, K. Sugihara: Design of a semi-autonomous underwater vehicle for intervention missions (SAUVIM). International Symposium on Underwater Technology - SSC , 1998

[3] Casalino, G., Caccia, M., Caiti, A., Antonelli, G., Indiveri, G., Melchiorri, C., and Caselli,S.: MARIS: A National Project on Marine Robotics for InterventionS. 22nd Mediterranean Conference of Control and Automation (MED),page:864 - 869,(June 2014).

[4] Simetti, E., Casalino, G., Torelli, S., Sperinde A. and Turetta,A.: Floating Underwater Manipulation: Developed Control Methodology and Experimental Validation within the TRIDENT Project. Journal of Field Robotics, volume 31(3):364385, (May 2014).

[5] Lane, D. M., Davies, J. B. C., Casalino, G., Bartolini, G., Cannata, G., Veruggio, G., Canals, M., Smith, C., O'Brien, D. J., Pickett, M., Robinson, G., Jones, D., Scott, E., Ferrara, A., Angelleti, D., Coccoli, M., Bono, R., Virgili, P., Pallas, R., and Gracia, E.: Amadeus: advanced manipulation for deep underwater sampling. IEEE Robot Automation Magazine, 4(4):34-45.(1997).

[6] Siciliano, B. and Slotine, J.-J. E.: A general framework for managing multiple tasks in highly redundant robotic systems. In Proc. Fifth Int Advanced Robotics 'Robots in Unstructured Environments', 91 ICAR. Conf, pages 1211-1216 (1991).

[7] Yoshikawa, T.: Manipulability of robotic mechanisms. Int. J. of Robotics Research, 4(1):3-9(1985).

[8] Prats, M.; Perez, J.; Fernandez, J.J.; Sanz, P.J.: An open source tool for simulation and supervision of underwater intervention missions. 2012 IEEE/RSJ International Conference on Intelligent Robots and Systems (IROS), pp. 2577-2582, (7-12 Oct. 2012).

[9] Antonelli, G. and Chiaverini, S.: Task-priority redundancy resolution for underwater vehicle-manipulator systems. In Proc. IEEE International Conference on Robotics and Automation, volume 1,pages 768-773(1998).

[10] Antonelli, G. and Chiaverini, S.: Fuzzy redundancy resolution and motion coordination for underwater vehicle-manipulator systems. IEEE Trans. on Fuzzy Systems, 11(1):109-120 (2003).

[11] Padir, T.: Kinematic redundancy resolution for two cooperating underwater vehicles with on-board manipulators. In Proc. IEEE Int Systems, Man and Cybernetics Conf, volume 4, pages 3137-3142(2005).

[12] Sentis, L. and Khatib, O.: Control of free-floating humanoid robots through task prioritization. In Proceedings of the 2005 IEEE International Conference on Robotics and Automation, Barcelona, Spain(2005).

[13] Sugiura, H., Gienger, M., Janssen, H., and Goerick, C.: Real-time collision avoidance with whole body motion control for humanoid robots. In Proc. IEEE/RSJ Int. Conf. Intelligent Robots and Systems IROS 2007, pages 2053-2058(2007).

[14] Casalino, G., Cannata, G., Panin, G., Caffaz, A.: Om a Two-Level Hierarchical Structure for the Dynamic Control of Multifingered Manipulation. In Proceedings of the 2001 IEEE International Conference on Robotics and Automation, Seoul, Korea(2001).